

The logo for IRIS AperTO, featuring the text "IRIS" in a large, white, serif font, "Aper" in a smaller, white, sans-serif font, and "TO" in a large, white, serif font, all set against a red rectangular background.

UNIVERSITÀ  
DEGLI STUDI  
DI TORINO

This is the author's final version of the contribution published as:

Ilaria Valente;Barbara Stella;Daniele L. Marchisio;Franco Dosio;Antonello A. Barresi. Production of PEGylated nanocapsules through solvent displacement in confined impinging jet mixers. JOURNAL OF PHARMACEUTICAL SCIENCES. 101 pp: 2490-2501.  
DOI: 10.1002/jps.23167

The publisher's version is available at:

<http://linkinghub.elsevier.com/retrieve/pii/S0022354915315422>

When citing, please refer to the published version.

Link to this full text:

<http://hdl.handle.net/2318/103335>

This full text was downloaded from iris - AperTO: <https://iris.unito.it/>

---

iris - AperTO

University of Turin's Institutional Research Information System and Open Access Institutional Repository

1 **Production of PEGylated nanocapsules through solvent-displacement in confined impinging jets**  
2 **mixers**

3 **Ilaria Valente<sup>1\*</sup>, Barbara Stella<sup>2</sup>, Daniele L. Marchisio<sup>1</sup>, Franco Dosio<sup>2</sup>, Antonello A. Barresi<sup>1</sup>**

4 <sup>1</sup>Politecnico di Torino, Dipartimento di Scienza dei Materiali e Ingegneria Chimica, Corso Duca degli Abruzzi  
5 24, 10129 Torino, Italy;

6 <sup>2</sup>Università degli Studi di Torino, Dipartimento di Scienza e Tecnologia del Farmaco, via Pietro Giuria 9,  
7 10125 Torino, Italy

8

9 **ABSTRACT:**

10 The growth of importance of nanocapsules (and other particulate systems) in different fields requires fast  
11 and reproducible methods for their production. Confined impinging jet mixers were successfully used for  
12 the production of nanospheres and are now tested for the first time for the production of nanocapsules.  
13 This work focuses on the understanding of formation mechanisms and on the quantification of the effect of  
14 the most important operating parameters involved in their production. Solvent displacement is employed  
15 here for the assembly of the nanocapsules by using a PEGylated derivative of cyanoacrylate as copolymer.  
16 A comparison with nanospheres obtained under the same operating conditions is also reported. Results  
17 show that the oil-to-copolymer mass ratio (MR) is the main factor affecting the final size distribution and  
18 that small nanocapsules are obtained only at low oil-to-copolymer MR. The effect of mixing is significant,  
19 proving that mixing of solvent and antisolvent also affects the final size distribution; this depends mainly on  
20 the inlet jet velocity, but the size of the mixer is also important. The Reynolds number may be useful to take  
21 this into account for geometrically similar systems. Quenching by dilution allows to stabilize the  
22 nanocapsules, evidencing the role of aggregation and ripening

23 **Keywords:**

24 Nanocapsules, nanospheres, copolymer nanoparticles, confined impinging jets mixer, nano-flash  
25 precipitation, solvent-displacement

26

27 (\*) corresponding author: Tel: +39-011-5644679, Fax: +39-011-5644699, Email: [ilaria.valente@polito.it](mailto:ilaria.valente@polito.it)

28

## 29 INTRODUCTION

30 In the last years, the pharmaceutical interest in nanotechnology has widen because of the  
31 possibilities it offers in releasing drug molecules, enhancing their therapeutic activity, reducing side  
32 effects, and increasing the lifetime of the drug *in vivo*. Different nanocarriers have been  
33 investigated, namely, liposomes, solid lipid particles, microparticles, and nanoparticles based on  
34 synthetic or natural polymers. Polymer nanoparticles include polymeric nanospheres and polymeric  
35 nanocapsules. In nanospheres, the drug is incorporated in the polymeric matrix, whereas polymeric  
36 nanocapsules have an inner liquid core surrounded by a polymeric layer, so that a large variety of  
37 drugs can be dissolved in the inner core, according to their solubility. The drug molecules inside the  
38 nanospheres are generally dispersed in the polymer matrix in a sort of solid solution but may also  
39 form a solid core coated by the polymer, whereas in nanocapsules they are dissolved in the liquid  
40 core; as a consequence, drug release occurs according to different mechanisms in nanospheres and  
41 nanocapsules. It depends on biodegradation and bioerosion of the polymer by enzymes and on drug  
42 diffusivity through the polymeric matrix, in the case of nanospheres, whereas in nanocapsules it  
43 depends also on the partitioning between the media inside and outside the polymeric shell.<sup>1</sup> In  
44 comparison to nanospheres, nanocapsules need a lower amount of polymer and can be loaded with  
45 larger amounts of drug, depending on the drug solubility in the inner liquid.<sup>2</sup> This work focuses on  
46 polymeric nanocapsules for pharmaceutical applications, but nanocapsules find wide use also in the  
47 cosmetic and agrochemical fields. The wide growth of their application requires innovative methods  
48 for faster production; the use of micromixers is here investigated for the first time.

49 Polymers from the family of poly(alkyl cyanoacrylates) (PACA) have been extensively used for the  
50 preparation of drug carriers. PACA nanoparticles are very common, thanks to their ability to  
51 achieve tissue targeting and enhance the intracellular penetration of drugs.<sup>3</sup> The amphiphilic  
52 copolymer poly(methoxy polyethylene glycol cyanoacrylate-*co*-hexadecyl cyanoacrylate)<sup>4</sup>,  
53 indicated as poly(MePEGCA-*co*-HDCA) in what follows, is used in this work. This kind of  
54 copolymer allows to obtain “stealth” nanocapsules, thanks to the polyethylene glycol (PEG) chains.  
55 In fact, a limit of standard polymer nanoparticles, without PEG chains, is that *in vivo* opsonins  
56 adsorb onto their surface and then nanoparticles can be recognized by macrophages and can be  
57 accumulated in liver and spleen. A PEG coating increases their blood lifetime because it creates an  
58 aqueous shell around the nanoparticle, which avoids opsonin adsorption and the subsequent  
59 macrophage uptake.

60 Polymer nanocapsules, as well as nanospheres, can be prepared both by polymerization  
61 methods<sup>5,6</sup> and from preformed polymer, by different mechanisms such as, for example, solvent  
62 displacement,<sup>7</sup> emulsion–diffusion,<sup>8</sup> double emulsification,<sup>9</sup> and so on. The different processes and

63 the characteristics of the nanocapsules produced have been recently compared.<sup>10</sup> In solvent  
64 displacement methods (also called interfacial deposition or flash nanoprecipitation), the polymer is  
65 prepared in a previous step, resulting in some advantages with respect to interfacial polymerization.  
66 In fact, solvent displacement allows to use polymers with controlled molecular weight, avoids the  
67 presence of residual monomers in solution, it is simpler and more reproducible, and it is easier to  
68 scale-up. Solvent displacement consists of mixing a water-miscible organic phase, containing the  
69 polymer, the oil, and generally the drug, with an aqueous phase. The organic phase is referred to as  
70 solvent, whereas water is the antisolvent. When the two phases are mixed together, the organic  
71 phase diffuses rapidly into the water, where it is soluble and where on the contrary the polymer, the  
72 oil, and the drug are insoluble. The rapid diffusion of the solvent in the antisolvent is the driving  
73 force in nanocapsules formation, inducing oily drops formation and the interfacial deposition of the  
74 polymer around the oily drops.

75 The overall process being very rapid, it is influenced by mixing and in order to obtain good mixing  
76 conditions, special micromixers must be used. Confined impinging jet mixers (CIJMs) provide  
77 optimum mixing conditions. Their use in nanosphere formation was extensively studied<sup>11–13</sup> and  
78 they were found to be very useful in controlling the final particle size.<sup>14</sup> CIJMs consist of two high  
79 velocity linear jets of fluid that collide inside a small chamber, whose size affects the overall mixing  
80 rate.

81 Mixing mechanism and nanoparticle formation in CIJMs, similar to the ones studied in this work,  
82 were analyzed in previous papers through computational fluid dynamics (CFD)  
83 simulations.<sup>15,16</sup> CFD simulations allow to quantify the mixing dynamics of the two inlet streams  
84 inside the mixing chamber. Three types of mixing mechanisms are generally present: macromixing  
85 at the mixer scale, mesomixing at the scale of the largest turbulent eddies, and micromixing at the  
86 molecular scale. Each step controls the next one and can be rate limiting. CIJMs limit the  
87 mesomixing time and ensure fast homogenization (i.e., short macromixing time) of the two fluids.  
88 Characteristic global mixing times in these equipments were calculated by CFD and are in the order  
89 of magnitude of milliseconds.<sup>17,18</sup>

90 In this work, the use of the CIJMs for the production of polymer nanocapsules suitable for  
91 pharmaceutical applications is investigated for the first time. As the mechanisms of nanocapsule  
92 formation are likely different from those of nanospheres, we are particularly interested in  
93 investigating the interplay between mixing and nanocapsules formation, with the precise scope of  
94 highlighting similarities and differences. Attention is paid to the control of nanocapsule size  
95 distribution. In fact, different applications translate into different requirements. For example, in the  
96 case of intravenous administration, nanocapsules have to be smaller than 300 nm. For other

97 applications, such as cosmetic<sup>19</sup> and food,<sup>20</sup> size limitations are different; therefore, the  
98 development of strategies to control the final nanocapsule size turns out to be very useful. Our work  
99 aims also at understanding if mixing can be used (also for nanocapsule) as an active parameter to  
100 control and tune the final size distribution.

101 It should be highlighted that no drug has been considered in this work. Although in the case of  
102 nanospheres, the absence or the presence of the drug can significantly alter the results (and can  
103 modify the particle structure), especially in terms of stability (as shown, for example, for  
104 doxorubicin-loaded polymer nanospheres<sup>21</sup>), in the case of nanocapsules, the situation seems to be  
105 very different, representing yet another difference between the two systems. In fact, the oil  
106 separates from the initial single-phase system through spinodal decomposition; no energetic barrier  
107 has to be overcome (as dictated by the Cahn–Hilliard equation) and molecular diffusion is the  
108 bottleneck. As the drug is generally hydrophobic and in low concentration (in comparison with the  
109 oil), drug molecules will likely move rapidly inside the oily drops. Indeed, a successive study with a  
110 drug is required to prove this last point and this simpler oil–polymer system will be used as  
111 reference.

112

113

## 114 **THEORETICAL BACKGROUND**

115 The formation of nanocapsules and nanospheres during solvent displacement is a complex process  
116 and many theories and interpretations have been presented in the literature. Knowledge of what  
117 happens at the molecular level is of primary importance for manipulating and controlling the overall  
118 process. Classical precipitation theory explains particle formation in three steps: nucleation,  
119 molecular growth, and particle aggregation.<sup>22</sup> Supersaturation is the driving force for particle  
120 formation and in solvent displacement processes, it is built up by mixing of the solvent and the  
121 antisolvent. As in this work we are interested in both nanospheres and nanocapsules, it is necessary  
122 to review and briefly discuss the theory presented in the literature for these two systems.

123 In the case of nanospheres, the copolymer and organic compound are dissolved in the solvent and  
124 when mixed with the antisolvent, particles are formed. Johnson and Prud'homme<sup>23</sup> describe  
125 nanosphere formation as the competition of two simultaneous phenomena: nucleation of drug  
126 particles and copolymer self-assembly. The two phenomena are characterized by different time  
127 scales and in order to allow the copolymer molecules to interact with (and to deposit on) the  
128 growing particles, the two time scales have to match one another. Typical operating conditions,  
129 used in the production of most of the organic drug particles, are characterized by extremely high

130 supersaturation, resulting in very small nucleus size, practically instantaneous nucleation, with very  
131 little energy barrier. It is also important to compare these time scales with the mixing time scale. It  
132 was in fact observed that faster mixing generally results in smaller drug particles with higher  
133 functionalization by the copolymer; however, once a certain limit is reached, no significant change  
134 in nanoparticle properties is observed. This is probably related to the development of a spatially  
135 independent self-similar state caused by the achievement of fully turbulent flow.

136 In the case of nanocapsules, the inner core of the particle consists instead of a lipophilic liquid  
137 (usually oil), which is insoluble in the mixture of solvent and antisolvent. Thus, in nanocapsule  
138 formation, two phenomena are involved: oily drop formation and polymer deposition around the  
139 oily drop. Oily drop formation takes place through spinodal decomposition (as dictated by the  
140 Cahn–Hilliard equation). Therefore, although due to the high supersaturation the nucleation process  
141 involved in nanosphere formation generates a very small energy barrier, some differences between  
142 nanospheres and nanocapsules, where on the contrary spinodal decomposition occurs spontaneously  
143 without any energy barrier, might be observed.

144 In addition, when solvent and antisolvent are mixed together, the oil dissolved in the solvent  
145 separates, resulting in drops which tend to coalesce. This can be prevented (as in the case of  
146 nanospheres) by the deposition of the copolymer around the drops; however, in the case of  
147 nanocapsules, copolymer reorientation on the interface might play a different role. In any case, also  
148 for nanocapsules, mixing efficiency is expected to be fundamental in order to have homogeneous  
149 and optimal conditions for the formation of very small drops and an even distribution of copolymer  
150 molecules around drops.

151 Some authors<sup>24,25</sup> have acknowledged the important contribution of the Gibbs–Marangoni effect  
152 on the formation of nanocapsules, in which the driving force is the difference in the interfacial  
153 tension between the solvent and the antisolvent. This effect is not considered in this work because it  
154 is important when nanocapsules are produced with the classical method, adding slowly the solvent  
155 to the aqueous phase. Using micromixers, such as CIJMs, under very intense turbulent mixing  
156 conditions, this effect is expected to be less important.

157

## 158 **MATERIALS AND METHODS**

159 The poly(MePEGCA-*co*-HDCA) copolymer was synthesized by condensation of the two monomers  
160 (MePEG cyanoacetate and *n*-hexadecyl cyanoacetate) in ethanol and dichloromethane. The ratio

161 between MePEG cyanoacetate/hexadecyl cyanoacetate was 1:4. The synthesis was carried out under  
162 the presence of formaldehyde and dimethylamine, as described in another work,<sup>17</sup> following the  
163 procedure of Peracchia et al.,<sup>26</sup> with some minor changes.

164 The copolymer was characterized in terms of its molecular weight, by using dynamic light  
165 scattering (DLS) and by resorting to the Debye theory, by differential scanning calorimetry and  
166 by <sup>1</sup>H NMR.<sup>17</sup> DLS characterization resulted in a molecular weight of about 4.37 kDa, whereas the  
167 two other characterizations confirmed the presence of the two monomers (the lipophilic one,  
168 HDCA, and the hydrophilic one, MePEGCA) and their approximate ratio of 1:4.

169 In all the experiments, Miglyol® 812N (a mixture of capric and caprylic acid) was used as liquid  
170 core (courtesy of Sasol Italy S.p.A). The solvent is Acetone Chromasolv (high-performance liquid  
171 chromatography grade), purchased by Sigma–Aldrich Italia (Milano). Milli-Q RG system by  
172 Millipore® (Billerica, MA, USA) was used to produce the ultrapure water employed in all the  
173 experiments.

174 Nanocapsules and nanospheres were prepared by solvent displacement. In nanocapsule  
175 precipitation, the copolymer together with Miglyol® was dissolved in acetone and then mixed with  
176 pure water, whereas in nanospheres, only the copolymer was dissolved in the solvent. Apart from  
177 this, the two preparations were identical. After mixing with water, the particulate system was  
178 immediately formed. As already mentioned, since the process is strongly influenced by mixing,  
179 CIJMs were used that ensure high turbulence levels and short mixing times. Precipitation was  
180 carried out with and without quenching, in order to highlight the possible influence of aggregation;  
181 to this purpose, the outlet of the mixer (8 mL containing equal volumes of acetone and water) was  
182 collected in a beaker containing 4 mL of water. Tests have been carried out in order to identify the  
183 best quenching volume ratio. When this is too small, it could be ineffective in stabilizing the system  
184 but when this is too large, it makes it impossible to use the sample for further characterization  
185 (unless extensive and therefore extremely time-consuming water evaporation is carried out). Four  
186 milliliters of water (corresponding to a 1:2 acetone–water final ratio in the mixture) was found to be  
187 a good trade-off, as quenching with larger volumes did not result in significantly different data, still  
188 resulting in reasonable final nanocapsule concentration.

189 The solubility of the copolymer for three water–acetone mixtures was studied. The investigated  
190 water volume fractions were 0.5, 0.66 (equivalent to 2/3), and 0.9, corresponding to the three  
191 conditions used in our experiments. In fact, samples without quenching result in mixtures of 0.5,  
192 whereas in quenched samples, the water is twice the acetone, resulting in 2/3. The last condition  
193 corresponds to a sample wherein the largest part of the acetone has been removed. These  
194 experiments were performed at 30°C.

195 In our laboratory set up, solvent solution and antisolvent were loaded into two different plastic  
196 syringes of 100 mL of volume and fed into the mixers by using a syringe pump (KDS200, KD  
197 Scientific, Holliston, MA, USA). The pump was calibrated in order to make sure that the imposed  
198 flow rate (FR) was actually delivered. Then, the solvent was removed by a rotating low-pressure  
199 evaporative device (Stuart® Rotary Evaporators). The possible azeotrope for the acetone–water  
200 mixture is in the acetone-rich region; therefore, complete removal of acetone is possible (as the  
201 starting point is an already water-rich solution). The effect of acetone removal on nanocapsules was  
202 quantified and found to be within the range of experimental uncertainty. Stability of the  
203 nanocapsule size after solvent removal was monitored by storing samples at 4°C for several weeks  
204 and measuring the nanocapsule size at regular time interval. No significant size changes were  
205 detected.

206 Four different CIJMs were used in this work. They all are similar but are characterized by different  
207 size of the inlet and outlet pipe and of the mixing chamber. A sketch is reported in Figure 1,  
208 whereas the detailed quotes are reported in Table 1. They are labeled in what follows as scale-down,  
209 CIJM-d1, scale-up (corresponding to three CIJMs exactly scaled-up by a geometric factor equal to  
210 two), and CIJM-d2 (corresponding to the same chamber size of CIJM-d1 but with bigger inlet pipe).  
211 The comparison of the results obtained with these four mixers allows to evidence scale-up and  
212 scale-down effects, as well as the effect of the chamber and inlet pipe size on the final size  
213 distribution.

214 Nanocapsules and nanospheres were characterized in terms of their size distribution (although  
215 reported data refer only to the mean size) and zeta potential and spherical shape was confirmed by  
216 Field Emission Scanning Electron Microscope (FESEM) pictures. The size of nanocapsules was  
217 determined by DLS (DLS, Zetasizer Nanoseries ZS90, Malvern Instrument, Worcestershire, UK)  
218 that measures accurately in the size range from 2 nm to 3  $\mu\text{m}$ . Zetasizer Nanoseries ZS90 does not  
219 use a movable detector but uses classical fixed detection arrangement at 90° to the laser and the  
220 center of the cell area. In DLS measurements, the intensity size distribution is converted by using  
221 the Mie theory to a volume size distribution. In order to obtain the volume size distribution, it is  
222 necessary to provide the instrument the refractive index of the material (which does not  
223 significantly influence the final result of the measurement) and of the dispersant. Before measuring,  
224 the sample was diluted to 1:100 in order to reduce the solid concentration. In DLS, it is important to  
225 have a sample with appropriate particle concentration; in fact, it has not to be too concentrated  
226 because each single photon should be scattered only once before reaching the detector, but it has to  
227 be concentrated enough to result in sufficient statistics. The parameters which assure the quality of  
228 the measurements (i.e., polydispersion index, correlation function parameter) were controlled for



229 each single sample and measurements were repeated when the quality criteria were not reached.  
230 Each sample was measured three times and the average value is reported in the figures. Thus, in the  
231 following figure, z-average values are reported.

232 The surface charge of nanoparticles was inferred through zeta potential measurements in water, by  
233 the same instrument, after dilution (1:10). In zeta potential measurements, the instrument measures  
234 the electrophoretic mobility, which is the velocity of a particle in an electric field. The zeta potential  
235 is then calculated from the Henry equation that makes use of the Smoluchowski approximation,  
236 valid for particles in aqueous samples.

237 All the experiments were performed after dissolving the copolymer and the oil in the acetone. No  
238 stabilizing agent was added to the aqueous phase as the PEGylated polymer can act as a stabilizer  
239 due to its amphiphilic nature.

240 In order to investigate the interplay between mixing and nanocapsule formation, experiments were  
241 carried out in a wide FR range up to 120 mL/min for both solutions. Results from our previous  
242 work<sup>17</sup> show that under these conditions, the mixers work under different fluid dynamics regimes.  
243 In fact, the flow is highly turbulent only at the highest FRs (larger than 40 mL/min for the smallest  
244 mixers and larger than 90 mL/min for the biggest mixers) and is instead transitional for the lowest  
245 FRs. In all cases, however, the outlet stream is well mixed, as also at relatively low FRs, good  
246 mixing performances are generally obtained. The reason for investigating the performance of these  
247 devices also at low FRs, when the flow is not fully turbulent, is to verify the possibility of using  
248 mixing as an operating parameter to control the final nanocapsule size.

249 In these experiments, the acetone solution contained 6 mg/mL of copolymer and 8  $\mu$ L/mL of oil  
250 (7.6 mg/mL), equivalent to an oil-to-copolymer mass ratio (MR) value of  $MR = 1.26$ . We  
251 performed the experiments both with and without quenching to understand the mechanism of  
252 nanocapsule formation and the main differences with respect to nanospheres. In some cases,  
253 experiments were repeated three times in order to quantify the experimental variability, reported  
254 together with the data in the form of error bars.

255 The effect of oil concentration on nanocapsule size was studied at four different oil concentrations:  
256 0 (i.e., nanospheres), 4.8  $\mu$ L/mL (4.56 mg/mL), 8  $\mu$ L/mL (7.6 mg/mL), and 15  $\mu$ L/mL (14.25  
257 mg/mL) with 6 mg/mL of copolymer concentration. The respective oil-to-copolymer MR was 0.76,  
258 1.26, and 2.37. These experiments were performed in all the CIJMs. Moreover, the same  
259 experiments were performed in the CIJM-d1, varying the copolymer concentration (10, 6, and 3.2  
260 mg/mL). In this case, the oil concentration was kept constant at 8  $\mu$ L/mL; in this way, the oil-to-  
261 copolymer MR was the same of the previous experiments (0.76, 1.26, and 2.37).

262 A further set of experiments, keeping constant the oil-to-copolymer mass ratio (MR), was also  
263 carried out. In this case, both copolymer and oil concentrations varied in order to check if it resulted  
264 in nanocapsules with similar size. The two MRs considered were 0.76 (with the following different  
265 concentrations: 4 mg/mL copolymer and 3.2  $\mu$ L/mL oil, 6 mg/mL copolymer and 4.8  $\mu$ L/mL oil, 10  
266 mg/mL copolymer and 8  $\mu$ L/mL oil) and 2.37 (3.2 mg/mL copolymer and 8  $\mu$ L/mL oil, 6 mg/mL  
267 copolymer and 15  $\mu$ L/mL oil). This set of experiments was carried out only in CIJM-d1 mixer.  
268 Both the FR and the inlet diameter ( $d_{in}$ ) of the mixer were varied in the experiments resulting in  
269 different mixing regimes inside the device. FR, velocity of the inlet jet ( $v_j$ ), and  $d_{in}$  are related  
270 through the following relationship:

$$271 \pi \frac{d_{in}^2}{4} v_j = FR, (1)$$

272 At the same FR, the fluid velocity is different in different mixers, resulting in different mixing  
273 efficiencies. According to Johnson and Prud'homme,<sup>27</sup> the overall mixing time ( $\tau_{mix}$ ) can be  
274 calculated as follows:

$$275 \tau_{mix} \propto v_j^{-3/2} (2)$$

276 when the flow is fully turbulent and, of course, different mixers are characterized by different  
277 residence times:

$$278 \tau_{res} = \frac{V_M}{FR} (3)$$

279 where  $\tau_{res}$  is the residence time and  $V_M$  is the volume of the mixer.

280

## 281 RESULTS AND DISCUSSION

282 Solubility tests revealed that the polymer residual concentration in the water–acetone mixture is  
283 significant when there is an equal amount of water and acetone and this amount slightly decreases  
284 when the water amount increases. A reduction in residual solubility is in fact detected when almost  
285 all the acetone (90%) is removed. Results are summarized in Table 2. This suggests that during  
286 acetone removal, additional polymer molecules can deposit on already formed nanocapsules and  
287 nanospheres. However, this amount does not significantly impact on the final particle size, as size  
288 measurements performed before and after removal (data not shown) highlighted very limited  
289 variations.

290 Nanocapsule formation was firstly investigated by comparing different mixers and different FRs  
291 (with and without quenching) and subsequently by comparing different initial compositions  
292 (copolymer and oil concentration). Results for the three CIJMs geometrically similar are reported in  
293 Figure 2. The figure shows the zeta potential and the mean particle size for nanocapsules prepared

294 with an acetone solution of 6 mg/mL of copolymer and 8  $\mu$ L/mL of oil (resulting in MR = 1.26) at  
295 different FR values, with and without quenching.

296 Let us first highlight the effect of the quenching water; if nanocapsules are not quenched, their final  
297 mean size (after solvent evaporation) is significantly larger; this general behavior will be observed  
298 in all the cases investigated, and will be discussed as follows.

299 A common trend for all the mixers can be observed: increasing the FR, faster mixing is achieved,  
300 resulting in smaller particles. It is also interesting to observe that it is the same for both the  
301 quenched and the nonquenched particles. The data seem to evidence a point after which further  
302 increases in FR has little effect; this is expected by previous works in similar fields. The goal of  
303 using special intensive mixers (such as the ones used in this work) is to ensure that the mixing time  
304 is fast enough (in comparison with the particle formation time) so that the system can be considered  
305 homogeneous. It is not completely correct to specify a single break point, as in the range  
306 considered; in fact, the size is affected by fluid dynamics in a similar way, but this is true on a  
307 logarithmic scale. The effect of a variation of the inlet FR is strong at low FRs (generally below 20  
308 mL/min), whereas it is very weak at higher FRs, generally larger than 40 mL/min. Results seem to  
309 show that mixing can also be used as an active parameter to control particle size. If one wants  
310 smaller particles, higher FRs (and faster mixing rates) should be used; on the contrary, if one wants  
311 bigger particles, smaller FRs (and slower mixing rates) should be used. This can be done until an  
312 effect of the wideness of the size distribution is detected. As simulations for a similar system show,  
313 in some cases there is a significant effect of mixing on particle size but a very limited one on  
314 polydispersity (especially when this is quantified as relative to the mean particle size). The  
315 combination of these two factors results in the possibility of playing with mixing only for the fine  
316 tuning of particle size, leaving almost unchanged relative polydispersity.

317 It must be said that at very low FR the uncertainty of the experimental data is relatively high,  
318 especially for the larger mixers, for which a lower reproducibility is observed; this may be a  
319 consequence of the fluid dynamic regime, as the inlet jets are laminar and thus the flow in the  
320 chamber is in the transitional region, with turbulence developing. In any case, it seems that the size  
321 increase that is observed, even when no quench is used, is similar in the whole range investigated,  
322 including the low FR region, thus confirming that the mixing performances of these devices are  
323 good also in the laminar regime.

324 In Figure 2, the performances of the three mixers are compared plotting the size of the nanocapsules  
325 obtained versus the inlet FR (the FR in each of the two inlets is considered), in order to evidence the  
326 influence of the size of the apparatus at constant throughput. The measured zeta potential is, as

327 average, between  $-30$  and  $-45$  mV, indicating that nanocapsules are stable from the electrochemical  
328 point of view. They reach lower values ( $-40$  and  $-50$  mV) if water dilution is carried out.

329 The scale-down mixer results in the smaller nanocapsules, probably due to the fact that it gives the  
330 best mixing conditions, at fixed FR. As scale-down mixer inlet jet diameter is  $0.5$  mm, the inlet  
331 stream can reach very high velocities, and as a consequence, high turbulent energy dissipation rates,  
332 and very short mixing times. But the inlet jet velocity is not the controlling variable, as shown in  
333 Figure 3; in fact, it can be noted that comparing the size obtained in the different mixers at the same  
334 inlet velocity, the conclusion is reversed, and the smallest nanocapsules are obtained in the scale-up  
335 mixer, whereas the scale-down mixer gives larger particles (and with higher energy costs). Only the  
336 quenched particle case is shown, but the behavior is similar (at least for the three-scaled mixers) for  
337 the nonquenched case. In these cases, the ratio between the inlet jet diameter and the chamber size  
338 is maintained constant, thus it is not possible to evidence which one of these geometrical variables  
339 eventually is more important, but it may be concluded that a larger size is surely favorable because  
340 it allows to increase throughput, reducing at the same time the final particle size (or eventually to  
341 obtain the same size at reduced jet velocity, and thus with lower energy input).

342

343 It is thus evident that the size of the apparatus plays a more complex role; if the Reynolds number is  
344 used to characterize the fluid dynamic conditions, and thus mixing, it is observed that the curves  
345 corresponding to the three mixers collapse onto a single one. Of course, Reynolds number can take  
346 into account only fluid dynamics similarity and only for geometrically similar devices, thus the  
347 behavior described above is observed only for the three-scaled mixers and for the same inlet  
348 concentrations of oil and polymer (that is for a fixed characteristic process time).

349 More complex to explain is the behavior of the CIJM-d2, which has the same chamber of the CIJM-  
350 d1, but larger inlet pipe diameters, equal to those of the scale-up device; in particular, significant  
351 differences are observed with and without quench. When nanocapsules are quenched, the size of the  
352 particles obtained, at a given FR, is approximately the same in the CIJM-d2 and in the scale-up  
353 mixer. It can be noted that in this case the inlet velocity is also the same, as the pipe diameter is  
354 equal (see also Fig. 3); this would suggest that the jet velocity is more relevant than the chamber  
355 size to determine mixing conditions. On the contrary, at a given jet velocity, smaller particles are  
356 obtained in the CIJM-d2 than in CIJM-d1; this might indicate that, for a given chamber volume, it is  
357 favorable to have a larger interaction zone of the two streams. It can be noted anyway that operating  
358 at the same jet velocity in the two considered mixers requires larger FRs in the one with larger pipe  
359 diameters (the CIJM-d2), and this leads to proportionally shorter residence times; thus, the smaller

360 size might be also a consequence of the reduced time for coalescence, and connected to a lower  
361 yield of the process.

362 If the outlet flow is not quenched, the behavior is different. At a given FR, the CIJM-d2 produces  
363 particles significantly larger than all the others, and in particular larger than the scale-up mixer;  
364 comparing the performances at a given inlet velocity, CIJM-d2 and CIJM-d1 produce nanocapsules  
365 of similar size. The comparison with the scale-up mixer evidences that in this case a larger chamber  
366 is favorable, as it allows to obtain smaller nanocapsules; as suggested by Johnson and  
367 Prud'homme,<sup>27</sup> what may be relevant is the ratio between the inlet pipe diameter and a characteristic  
368 chamber dimension and this value must not be too large to allow the mixing to be confined within  
369 the chamber. It is possible that in CIJM-d2, the particle formation process is not completed in the  
370 mixer, and this can explain the significant size increase observed in case of nonquenched  
371 nanocapsules; the CFD simulations carried out in a previous work for the same geometry confirm  
372 that the mixing process (at very low FRs) may be not complete.<sup>18</sup> This fact may be also responsible  
373 for the larger experimental uncertainty that is observed in the test carried out in the CIJM-d2.

374 The influence on the mean nanocapsule size of the inlet pipe diameter, for mixers with the same  
375 chamber volume, is shown in Figure 4; in this case, the data are plotted considering the inlet jet  
376 Reynolds number (for an inlet jet with average properties of the mixed liquid streams). It can be  
377 noted that in case of quenched nanocapsules, a unique curve is obtained (and as discussed before,  
378 this is the same curve valid for all the mixers in these concentration conditions), whereas for  
379 nonquenched ones, larger sizes are obtained in the CIJM-d2, as discussed before. Figure 4 allows  
380 also to compare the experimental uncertainty in the case of quenched and nonquenched processes;  
381 in the latter case, it is significantly higher. Zeta potential measurements (not shown) result in values  
382 slightly lower than  $-30$  mV.

383

384 These results show the feasibility of CIJMs for the production of nanocapsules and prove that fast  
385 mixing is needed in order to control nanocapsules size and in order to guarantee high  
386 reproducibility. Better mixing conditions allow the formation of smaller oily drops and a better  
387 coverage by the copolymer, resulting in smaller particles. Moreover, results show that quenching is  
388 an important factor and cannot be avoided if nanocapsules with controlled characteristics are  
389 desired. It may be also concluded that the process can be scaled using the Reynolds number, at least  
390 for geometrically similar devices; the relative size of inlet pipes and chamber has shown to affect  
391 the process, but its influence on final nanocapsule size is complex, and cannot be taken into account  
392 with a simple relationship, such as that proposed for the mixing time in literature.<sup>27</sup> Also the  
393 influence of the mixing time will require further work to be quantified in the case of this specific

394 application. In fact, the results obtained confirm that process kinetics and mixing interact and when  
395 reducing the mixing time, smaller particles are obtained. However, modifications of the mixer size  
396 and geometry cannot be taken into account simply by the variation in the mixing time estimated in  
397 the different mixing devices, even for the same inlet polymer and oil concentrations. In fact, using  
398 the mixing times estimated by CFD simulations<sup>18</sup> for the different mixers to correlate the particle  
399 size obtained, it is not possible to obtain a unique curve for the runs obtained in different mixers.

400 The effect of oil concentration on nanocapsule formation was also investigated. At a constant  
401 copolymer concentration of 6 mg/mL, the oil concentration was varied between zero (resulting in  
402 nanospheres) and a maximum value. Data are collected in Figure 5, where the results obtained for  
403 four different oil-to-copolymer MRs are reported for each mixer; the data are plotted versus the  
404 Reynolds number, on the basis of the results discussed in the previous parts of this work, and as the  
405 experiments were carried out in the same flow rate range for the different mixers, obviously the  
406 extension of the jet Reynolds number range investigated is different. The results confirm that for  
407 every set of concentrations, a single curve is obtained for the different scaled mixers (in fact, the  
408 approximation curve drawn in the different graphs of the figure is this common line), whereas a  
409 behavior similar to that discussed before is observed for the CIJM-d2. These conclusions are  
410 generally valid also for other polymer concentrations, but as it will be shown in the following, for  
411 very low polymer concentrations, the formation of nanocapsules may be difficult.

412 As a general trend, it is possible to state that decreasing the oil-to-copolymer MR, the mean particle  
413 size decreases. That can be due to the fact that when the oil-to-copolymer MR increases, there is not  
414 enough copolymer to cover a larger surface area, resulting in bigger nanocapsules.

415 Each experiment at a given oil-to-copolymer MR was repeated with and without quenching water.  
416 Quenching reduces the final nanocapsule size, but the effect is stronger at higher ratios, where there  
417 is a lower amount of copolymer. As already mentioned, the operation of quenching allows to stop  
418 nanocapsule evolution and freeze them as they are immediately after exiting the CIJM. In fact,  
419 quenching dilutes the residual polymer concentration and the particulate system decreasing the  
420 probability of nanocapsule collision and further growth. If we compare the results at different oil-to-  
421 copolymer MRs, it is clear that the size increase is more relevant at high MR values, where there is  
422 less copolymer to cover the oily drops. As a matter of fact, the results obtained at  $MR = 0.76$   
423 present a very small difference with or without quenching. This suggests that the copolymer coating  
424 has an important role in stabilizing the suspensions and avoiding nanocapsule aggregation and  
425 coalescence.

426 In Figure 5 also nanospheres produced under similar operating conditions are shown for  
427 comparison; the size is always much smaller than that obtained in nanocapsules, which is mainly

428 determined by the size of the oil drops formed, suggesting that size increase can take place for  
429 further aggregation of copolymer molecules from the solution and not for the collision of the  
430 nanospheres.

431 In comparison to nanospheres ( $MR = 0$ ), where there is no oil inside, in nanocapsule, the energy  
432 barrier that has to be overcome due to repulsion forces in case of aggregation seems to be lower due  
433 to the presence of the oil. Thus, the stability of the nanocapsule suspension could be related with the  
434 thickness of the copolymer wall formed. This will surely decrease if the oil-to-copolymer MR is  
435 increased and in the case considered is the largest at  $MR = 0.76$ . Moreover, we can assume that  
436 good mixing allows more copolymer to be available for covering oily drops.

437 As noted in Figure 2, particle size does not significantly change when working with FR values  
438 greater than 40 mL/min. That probably happens because the system reaches good mixing  
439 conditions, which guarantee small particle size. Comparison with the data shown in  
440 Figure 5 highlights an additional element. If we consider particle size obtained at Reynolds numbers  
441 greater than 1000 (i.e., high mixing efficiency), the differences among the mixers are very small for  
442 each MR investigated. In fact, the variation of particle size at each MR is smaller than 40 nm,  
443 suggesting that the effect of the mixer geometry is very low when the highest mixing efficiency is  
444 reached. Moreover, results are very reproducible at high mixing efficiency, on the contrary to what  
445 happens under laminar conditions, where the data from different geometries are more scattered.

446 In Figure 6, zeta potential is shown as a function of the size for nanocapsules obtained with  
447 different mixers, the FRs and oil-to-copolymer ratios. As it is possible to see no significant  
448 differences are detectable depending on the mixers used, showing that both nanocapsules and  
449 nanospheres present the same superficial properties independently on the mixer used, small  
450 differences seem to exist between nanocapsules and nanospheres, but no significant differences are  
451 noted among nanocapsules obtained at different MR. The fact that the presence of the oil does not  
452 impact the final zeta potential value of nanocapsules could be interpreted as a proof of the fact that  
453 the oil stays inside the copolymer shell. This hypothesis is supported by preliminary experimental  
454 evidences obtained with X-ray photoelectron spectroscopy<sup>28</sup> and will be reported in future  
455 communications.

456 As previously mentioned, the copolymer concentration was also varied, keeping constant the oil  
457 concentration. Experiments were performed only in CIJM-d1 with and without quenching and all  
458 the previous trends were confirmed, as shown in Figure 7 where the data are plotted versus  
459 Reynolds as in previous cases. It may be noted that at low polymer concentration, the size of the  
460 nanocapsules measured becomes extremely large, and it is evident that the situation must be  
461 different from the other cases, where a proportional variation of the polymer had a relatively small

462 effect. Probably, under these conditions, the polymer quantity available for the formation of the  
463 copolymer shell is too small, and the forming nanocapsules collapse; further work will be necessary  
464 to investigate what happens under these limiting conditions.

465 Figure 8 shows results for nanocapsules obtained with CIJM-d1 for different initial oil and  
466 copolymer concentrations, but at the same relative MR to investigate the role of the total  
467 concentration of both copolymer and oil.

468 Results confirm that the copolymer concentration can play also an important role in the final  
469 nanocapsule size, as it stabilizes oily drops and prevent further coalescence. In particular, they  
470 clearly show that at MR lower than one, the total concentration of polymer and oil is not important,  
471 but it is their MR that determines the final size, indicating that the copolymer is able to block oily  
472 drops growth by surrounding them; at higher MRs, results depend on the polymer concentration. As  
473 already mentioned, working at high mixing intensity (Reynolds numbers greater than 1000) the  
474 mean particle size is, on average, between 170 and 280 nm, depending on the mixer and on the MR.  
475 The only data point which does not fall within this range was obtained at MR 2.37 with a  
476 copolymer concentration of 3.2 mg/mL and oil concentration of 8  $\mu$ L/mL. This data set shows a  
477 mean particle size drastically larger than that for samples obtained under similar operating  
478 conditions, even in case of quench; the relative increase observed for nonquenched particles, then,  
479 is very relevant. Moreover, the solubility data already discussed show that there is a copolymer  
480 amount remaining in the solution (0.2 g/L in acetone–water mixture at 90% of water) that has to be  
481 subtracted from the initial copolymer concentration to give the effective available copolymer  
482 amount. This is naturally more important at low initial copolymer concentrations, as in the case of  
483 3.2 mg/mL.

484 To conclude, this second data set shows that increasing the copolymer amount, nanocapsule size  
485 decreases and probably copolymer wall thickness increases. Quenching is useful in stabilizing the  
486 system, preventing further aggregation especially when the copolymer amount is lower (and  
487 probably the copolymer wall is thinner), but below a certain polymer concentration, nanocapsules  
488 of controlled size cannot be obtained; the limit conditions, that probably depend on residual  
489 polymer solubility in the liquid mixture, and on process yields, require further investigation.

490

## 491 **CONCLUSIONS**

492 We synthesized a PEGylated cyanoacrylate amphiphilic copolymer, in order to prepare  
493 nanocapsules for pharmaceutical applications. PEGylated copolymers are very useful in the  
494 pharmaceutical field as they increase the blood lifetime of particulate carriers. At the same time,



495 they are advantageous as they act as stabilizers, allowing to work without additional stabilizing  
496 agents, thus reducing the costs and avoiding possible toxicity problems.

497 Nanocapsules were prepared for the first time using CIJMs. These devices provide good mixing and  
498 were already used for obtaining nanoparticles of different materials. The mechanisms involved in  
499 nanocapsule formation inside these devices are still not completely clear, as nanocapsules are a  
500 complex system with more variables involved. The influence of mixer geometry on nanocapsule  
501 formation needs more investigation, especially to understand how the overall mixing time affects  
502 the final nanocapsule size and copolymer distributions.

503 The results reported in this work demonstrate that CIJMs can be successfully used in nanocapsule  
504 production and represent possibility route for their continuous production. Different types of  
505 nanoparticles are now reaching the clinical trial level; therefore, a continuous route for producing  
506 them with reproducible characteristics is highly desirable.

507 Further investigations on the pharmaceutical properties of nanoparticles produced by this way are  
508 required, in order to give a complete evaluation of the product and of the system together with the  
509 limiting operating conditions that allow to obtain stable nanocapsules.

510

511

512 **REFERENCES**

- 513 1) Ammoury N, Fessi H, Devissaguet JP, Puisieux F, Benita S. 1990. In vitro release kinetic pattern  
514 of indomethacin from poly(d,l-Lactide) nanocapsules. *J Pharm Sci* 79:763–767.
- 515 2) Stella B, Arpicco S, Rocco F, Marsaud V, Renoir JM, Cattel L, Couvreur P. 2007. Encapsulation  
516 of gemcitabine lipophilic derivatives into polycyanoacrylate nanospheres and nanocapsules.  
517 *Int J Pharm* 344:71–77.
- 518 3) Vauthier C, Labarre D, Ponchel G. 2007. Design aspects of poly(alkylcyanoacrylate)  
519 nanoparticles for drug delivery. *J Drug Target* 15:641–663.
- 520 4) Peracchia MT, Gref R, Minamitake Y, Domb A, Lotan N, Langer R. 1997. PEG-coated  
521 nanospheres from amphiphilic diblock and multiblock copolymers: Investigation of their drug  
522 encapsulation and release characteristics. *J Control Release* 46:223–231.
- 523 5) Bouchemal K, Briancon S, Fessi H, Chevalier Y, Bonnet I, Perrier E. 2006. Simultaneous  
524 emulsification and interfacial polycondensation for the preparation of colloidal suspensions of  
525 nanocapsules. *Mater Sci Eng C* 26:472–480.
- 526 6) Pitaksuteepong T, Davies NM, Tucker IG, Rades T. 2002. Factors influencing the entrapment of  
527 hydrophilic compounds in nanocapsules prepared by interfacial polymerisation of water-in-oil  
528 microemulsions. *Eur J Pharm Biopharm* 53:335–342.
- 529 7) Peracchia MT, Vauthier C, Desmaele D, Gulik A, Dedieu JC, Demoy M, d'Angelo J, Couvreur  
530 P. 1998. Pegylated nanoparticles from a novel methoxypolyethylene glycol cyanoacrylate  
531 hexadecyl cyanoacrylate amphiphilic copolymer. *Pharm Res* 15:550–556.
- 532 8) Moinard-Checot D, Chevalier Y, Briancon S, Beney L, Fessi H. 2008. Mechanism of  
533 nanocapsules formation by the emulsion-diffusion process. *J Colloid Interface Sci* 317:458–  
534 468.
- 535 9) Garti N. 1997. Double emulsions—Scope, limitations and new achievements. *Colloids Surf A-  
536 Physicochemical Eng Aspects* 123:233–246.
- 537 10) Mora-Huertas CE, Fessi H, Elaissari A. 2010. Polymer-based nanocapsules for drug delivery.  
538 *Int J Pharm* 385:113–142.

- 539 11) Marchisio DL, Rivautella L, Barresi AA. 2006. Design and scale-up of chemical reactors for  
540 nanoparticle precipitation. *AIChE J* 52:1877–1887.
- 541 12) Gavi E, Marchisio DL, Barresi AA. 2008. On the importance of mixing for the production of  
542 nanoparticles. *J Dispersion Sci Technol* 29:548–554.
- 543 13) Gavi E, Marchisio DL, Barresi AA, Olsen MG, Fox RO. 2010. Turbulent precipitation in  
544 micromixers: CFD simulation and flow field validation. *Chem Eng Res Des* 88:1182–1193.
- 545 14) Lince F, Marchisio DL, Barresi AA. 2008. Strategies to control the particle size distribution of  
546 poly- $\epsilon$ -caprolactone nanoparticles for pharmaceutical applications. *J Colloid Interface Sci*  
547 322:505–515.
- 548 15) Lince F, Marchisio DL, Barresi AA. 2009. Smart mixers and reactors for the production of  
549 pharmaceutical nanoparticles: Proof of concept. *Chem Eng Res Des* 87:543–549.
- 550 16) Gavi E, Rivautella L, Marchisio DL, Vanni M, Barresi AA, Baldi G. 2007. CFD modelling of  
551 nano-particle precipitation in confined impinging jet reactors. *Chem Eng Res Des* 85:735–  
552 744.
- 553 17) Lince F, Bolognesi S, Marchisio DL, Stella B, Dosio F, Barresi AA, Cattel L. 2010. Preparation  
554 of poly(MePEGCA-co-HDCA) nanoparticles with confined impinging jets reactor:  
555 Experimental and modelling study. *J Pharm Sci* 100:2391–2405.
- 556 18) Lince F, Marchisio DL, Barresi, AA. 2011. A comparative study for nanoparticle production  
557 with passive mixers via solvent-displacement: Use of CFD models for optimization and  
558 design, *Chem Eng Process* 50:356–368.
- 559 19) Alvarez-Roman R, Barre G, Guy RH, Fessi H. 2001. Biodegradable polymer nanocapsules  
560 containing a sunscreen agent: Preparation and photoprotection. *Eur J Pharm Biopharm*  
561 52:191–195.
- 562 20) Zambrano-Zaragoza ML, Mercado-Silva E, Gutiérrez-Cortez E, Castaño-Tostado E, Quintanar-  
563 Guerrero D. 2011. Optimization of nanocapsules preparation by the emulsion–diffusion  
564 method for food applications. *Food Sci Technol* 44:1362–1368.

- 565 21) Lince F, Bolognesi S, Stella B, Marchisio DL, Dosio F. 2011. Preparation of polymer  
566 nanoparticles loaded with doxorubicin for controlled drug delivery. *Chem Eng Res Des*  
567 89:2410–2419.
- 568 22) Horn D, Rieger J. 2001. Organic nanoparticles in the aqueous phase—Theory, experiment, and  
569 use. *Angew Chem Int Ed Engl* 40:4330–4361.
- 570 23) Johnson BK, Prud'homme RK. 2003. Flash NanoPrecipitation of organic actives and block  
571 copolymers using a confined impinging jets mixer. *Aust J Chem* 56:1021–1024.
- 572 24) Fessi H, Puisieux F, Devissaguet JPh, Ammoury N, Benita S. 1989. Nanocapsule formation by  
573 interfacial deposition following solvent-displacement. *Int J Pharm* 55:R1–R4.
- 574 25) Quintanar-Guerrero D, Allemann E, Fessi H, Doelker E. 1998. Preparation techniques and  
575 mechanisms of formation of biodegradable nanoparticles from preformed polymers. *Drug Dev*  
576 *Ind Pharm* 24:1113–1128.
- 577 26) Peracchia MT, Desmaele D, Couvreur P, d'Angelo J. 1997. Synthesis of a novel poly(MePEG  
578 cyanoacrylate-co-alkyl cyanoacrylate) amphiphilic copolymer for nanoparticle technology.  
579 *Macromolecules* 30:846–851.
- 580 27) Johnson BK, Prud'homme RK. 2003. Chemical processing and micromixing in confined  
581 impinging jets. *AIChE J* 49:2264–2282.
- 582 28) Valente I, Celasco E, Marchisio DL, Barresi AA. 2011. Nanoprecipitation in confined  
583 impinging jets mixers: Production and characterization of pegylated nanoparticles for  
584 pharmaceutical use. *Proceedings of 18th International Symposium on Industrial*  
585 *Crystallization*; September 13–16, 2011; Zurich, Switzerland, 172–173.
- 586

587

Mixer	$d_{in}$ (mm)	$d_{out}$ (mm)	$D_c$ (mm)	Volume (mm <sup>3</sup> )
Scale-down	0.5	1	2.4	22.5
CIJM-d1	1	2	4.8	180.3
Scale-up	2	4	9.8	1288.3
CIJM-d2	2	2	4.8	180.3

588

589 **Table 1. Geometrical details of the CIJMs used for the experiments.**

590

591

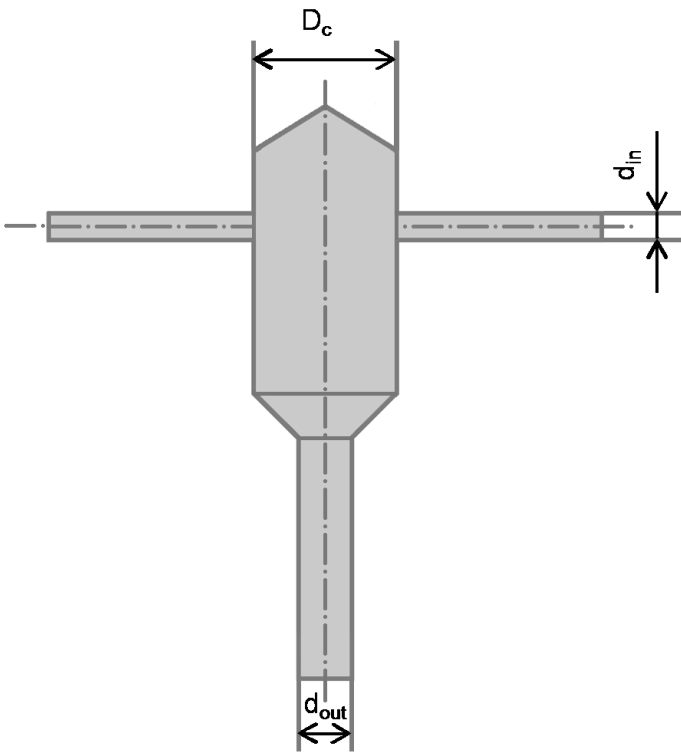
Water Volume Fraction	0.5	0.66	0.9
g/L	0.45	0.4	0.243

592

593 **Table 2. Polymer Solubility at Different Composition of the Water–Acetone Mixture**

594

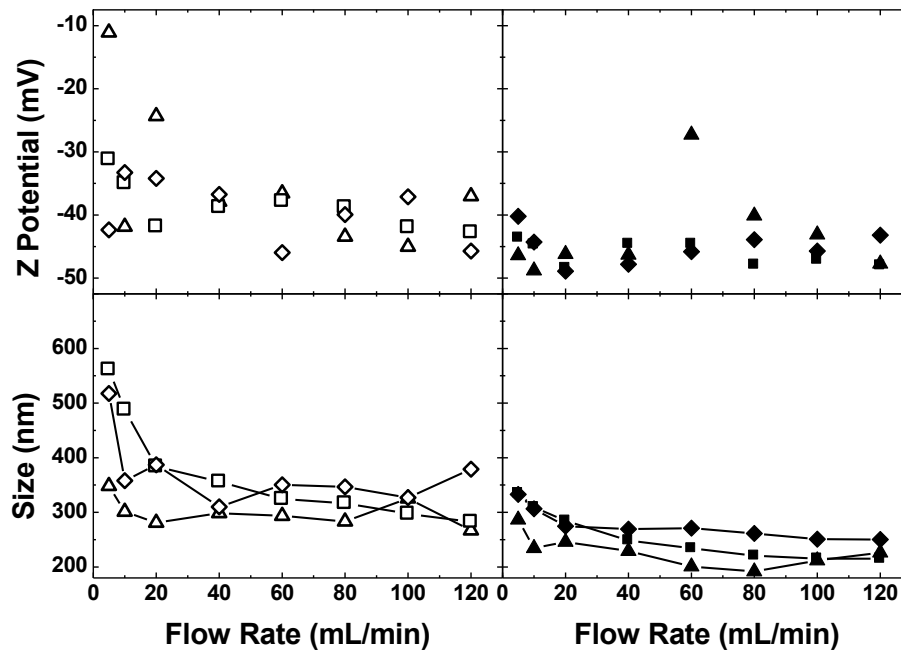
595



596

597 **Figure 1. Sketch of the CIJM used in this work.**

598

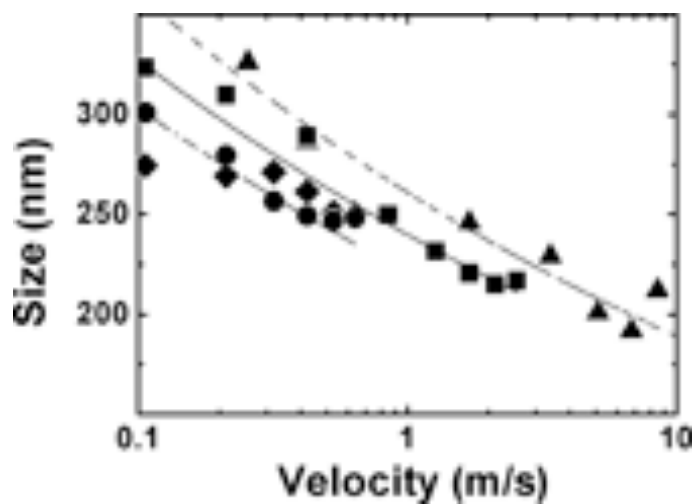


600

601 Figure 2. Mean particle size (bottom) and zeta potential (top) versus the flow rate for nanocapsules obtained  
 602 without quenching water (left, open symbols) and with quenching water (right, filled symbols) for different  
 603 mixers: scale down ( $\Delta$ ,  $\blacktriangle$ ), CIJM-d1 ( $\square$ ,  $\blacksquare$ ) and scale up ( $\diamond$ ,  $\blacklozenge$ ). Experiments at constant polymer (6 mg/mL)  
 604 and oil (8  $\mu$ L/mL) concentration (MR = 1.26).

605

606



607

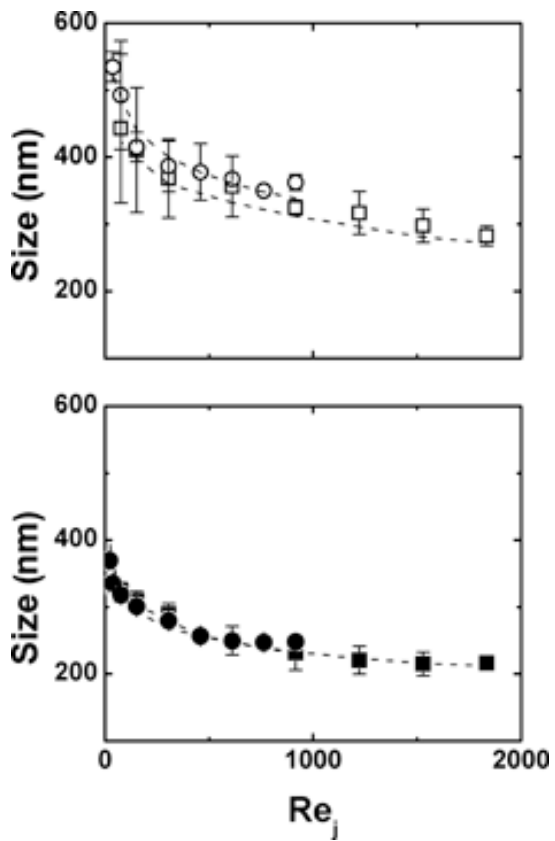
608 **Figure 3. Mean particle size versus the inlet stream velocity for nanocapsules obtained with different CIJMs:**  
 609 **scale-down mixer (▲), CIJM-d1 mixer (▪), scale-up mixer (◆), and CIJM-d2 mixer (●). Experiments at constant**  
 610 **polymer (6 mg/mL) and oil (8  $\mu$ L/mL) concentration (MR = 1.26).**

611

612



613



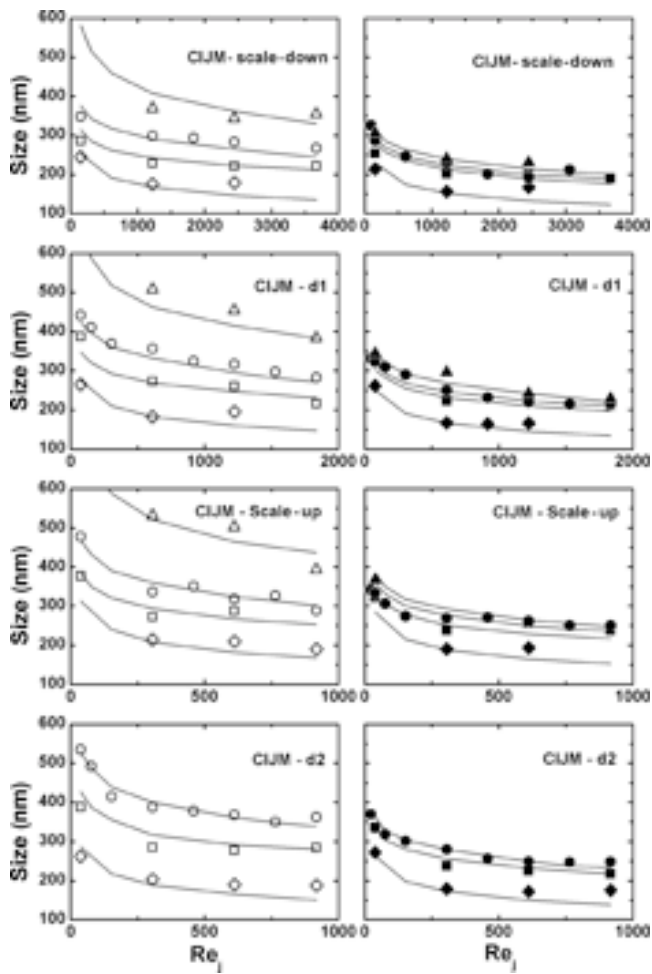
614

615 **Figure 4. Mean particle size versus the jet Reynolds number for nanocapsules obtained without quenching water**  
616 **(top, open symbols) and with quenching water (bottom, filled symbols) for CIJMs characterized by different**  
617 **inlet pipes and same mixing chamber: CIJM-d1 (□,▪), CIJM-d2 (○,•). Experiments at constant polymer (6**  
618 **mg/mL) and oil (8 μL/mL) concentration (MR = 1.26).**

619

620

621

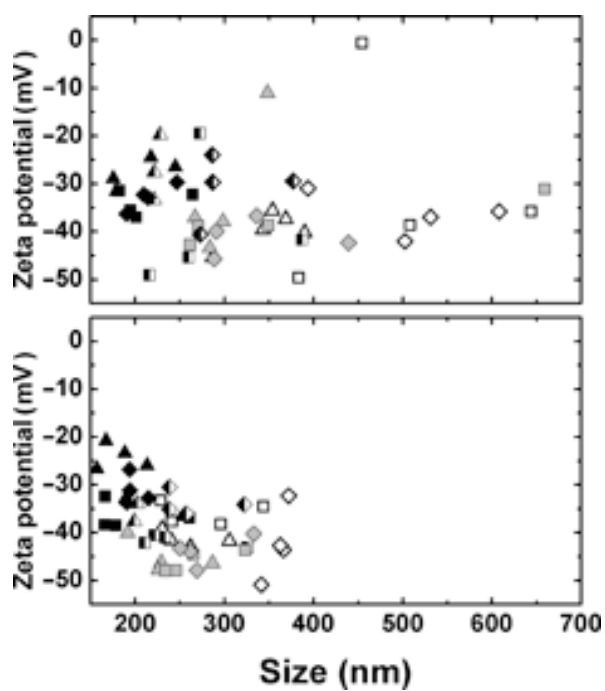


622

623 **Figure 5. Mean particle size versus the jet Reynolds number for nanocapsules and nanospheres obtained at four**  
 624 **different oil-to-copolymer mass ratios, MR = 0 ( $\diamond, \blacklozenge$ ), MR = 0.76 ( $\square, \blacksquare$ ), MR = 1.26 ( $\circ, \bullet$ ), and MR = 2.37 ( $\triangle, \blacktriangle$ )**  
 625 **without quenching (left, open symbols) and with quenching (right, filled symbols) for (from top to bottom) scale-**  
 626 **down, CIJM-d1, scale-up, and CIJM-d2. Constant polymer concentration (6 mg/mL).**

627

628



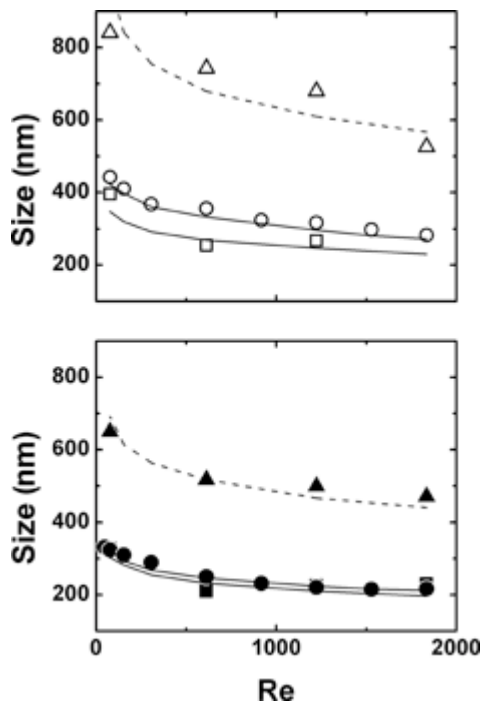
629

630 Figure 6. Zeta potential as a function of particle size obtained with different mixers: scale-down (triangle),  
 631 CIJM-d1 (square), and scale-up (rhomb). Top graph: particles without quenching. Bottom graph: particles with  
 632 quenching. Both nanospheres and nanocapsules are present: nanospheres (black), nanocapsules at MR = 0.76  
 633 (half black), nanocapsules at MR = 1.26 (light gray), and nanocapsules at MR = 2.37 (white).

634

635

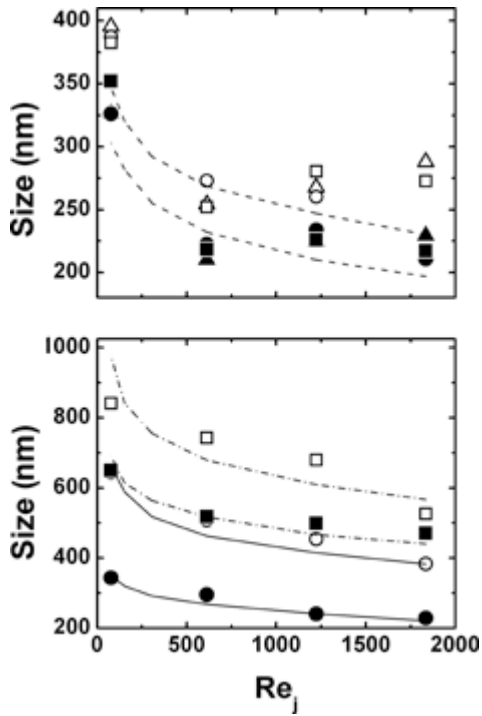
636



637

638 Figure 7. Mean particle size versus the jet Reynolds number for nanocapsules obtained at constant oil  
 639 concentration (8  $\mu\text{L}/\text{mL}$ ) and at copolymer concentration of 10 mg/mL (MR = 0.76,  $\square, \blacksquare$ ), 6 mg/mL (MR = 1.26,  
 640  $\circ, \bullet$ ), and 3.2 mg/mL (MR = 2.37,  $\triangle, \blacktriangle$ ) in CIJM-d1 without quenching (open symbols) and with quenching (filled  
 641 symbols).

642



643

644 **Figure 8. Mean particle size versus the jet Reynolds number for nanocapsules obtained with CIJM-d1 without**  
 645 **quenching (open symbol) and with quenching (filled symbol) at two different constant oil-to-copolymer mass**  
 646 **ratio for different copolymer and oil concentrations; upper graph: MR = 0.76 with 4 mg/mL copolymer and 3.2**  
 647 **μL/mL oil (□,•), 6 mg/mL copolymer and 4.8 μL/mL oil (○,•), 10 mg/mL copolymer, and 8 μL/mL oil (□,□);**  
 648 **lower graph: MR = 2.37 with 3.2 mg/mL copolymer and 8 μL/mL oil (□,•,——), 6 mg/mL copolymer, and 15**  
 649 **μL/mL oil (○,•, ——).**

650